

A scaling law for interstellar depletions

Giovanni Vladilo

Osservatorio Astronomico di Trieste, Via G.B. Tiepolo 11, I-34131 Trieste

vladilo@ts.astro.it

ABSTRACT

An analytical expression is presented that allows gas-to-dust elemental depletions to be estimated in interstellar environments of different types, including Damped Ly α systems, by scaling an arbitrary depletion pattern chosen as a reference. As an improvement on previous work, the scaling relation allows the dust chemical composition to vary and includes a set of parameters which describe how sensitive the dust composition is to changes in both the dust-to-metals ratio and the composition of the medium. These parameters can be estimated empirically from studies of Galactic and extragalactic depletion patterns. The scaling law is able to fit all the typical depletion patterns of the Milky Way ISM (*cold disk*, *warm disk*, and *warm halo*) with a single set of parameters, by only varying the dust-to-metals ratio. The dependence of the scaling law on the abundances of the medium has been tested using interstellar observations of the Small Magellanic Cloud (SMC), for which peculiar depletion patterns have been reported in literature. The scaling law is able to fit these depletion patterns assuming that the SMC relative abundances are slightly non solar.

Subject headings: ISM: abundances — ISM: dust — Galaxies: abundances — Galaxies: Magellanic Clouds — QSO: absorption systems

1. Introduction

It is well known that elemental abundances measured in the interstellar gas of the solar vicinity are generally depleted with respect to the solar values (Morton 1974; Jenkins, Savage & Spitzer 1986). The commonly accepted interpretation of this depletion effect is that a fraction of these elements is not detected in the gas because it is locked into dust grains. Elemental depletions are estimated by comparing the abundances measured in the gas with the abundances of the medium (gas plus dust). Intrinsic solar abundances are usually adopted in local interstellar studies, even though the interstellar abundance standard is not yet firmly established (Savage & Sembach 1996, hereafter SS96; Sofia & Meyer 2001). Different elements may have very different values of depletion, the so called "refractory" elements being almost completely in dust form. In addition, elemental depletions can vary significantly among different lines of sight. In spite of this complex

behavior, interstellar regions with similar physical conditions are characterized by similar depletions (Spitzer 1985; Jenkins et al. 1986). In the Galactic disk the cold gas has higher depletions than the warm gas; in the halo the warm gas shows even lower depletions (SS96).

Elemental depletions constitute an important piece of information for solving the complex puzzle of the origin and evolution of interstellar dust (Tielens & Allamandola 1987 and refs. therein). Studies of depletions in the Galaxy and in the Magellanic Clouds (MCs) have received new impulse (Roth & Blades 1995; Welty et al. 1997, 2001) owing to their importance in the interpretation of abundance patterns measured in the QSO absorbers of highest H I column density, namely the Damped Ly α systems (DLAs). These systems originate in intervening galaxies or protogalaxies and their abundances yield unique information on galactic chemical evolution at different redshifts (Lu et al. 1996; Prochaska & Wolfe 1999; Molaro

et al. 2000). The evidence that dust depletion may significantly affect the abundances of DLAs is quite compelling (Pettini et al. 1994; Lauroesch et al. 1996; Hou et al. 2001; Prochaska & Wolfe 2002). In order to cope with the problem of depletion in DLAs some authors have concentrated on studies of non-refractory elements (Pettini et al. 1997; Centurion et al. 2000; Vladilo et al. 2000) and of systems with small dust content (Pettini et al. 2000, Molaro et al. 2000). At the same time, formalisms have been developed to quantify the effect of dust depletions on DLA abundances (Kulkarni et al. 1997; Vladilo 1998; Savaglio, Panagia & Stiavelli 2000). These formalisms assume that the dust in DLAs is similar to Galactic interstellar dust. Depletions in DLAs have been modeled scaling Galactic depletions by allowing variations of the dust-to-metals ratios, but not of the dust chemical composition. In addition, the fact that the dust composition may be affected by variations of the intrinsic abundances of the intervening galaxies has not been considered.

In this work a scaling law of interstellar depletions is derived that allows the dust chemical composition to vary according to changes in the dust-to-metals ratio and/or to changes in the overall abundances of the medium (Section 2). Rather than assuming *ad hoc* types of dust, a set of parameters is introduced to describe how sensitive the dust composition is to changes in the physical and chemical properties of the medium. In Sections 3 and 4 it is shown that such parameters can be estimated from Galactic and extragalactic interstellar data. The conclusions are summarized in Section 5.

2. A scaling law for interstellar depletions

The interstellar depletion of an element X is usually defined as

$$D_x = \log \left(\frac{N_x}{N_H} \right)_g - \log \left(\frac{X}{H} \right)_m, \quad (1)$$

where N_x and N_H are the column densities measured in the gas (Spitzer 1978) and $(\frac{X}{H})_m$ is the abundance in the medium (gas plus dust). In Galactic studies one usually takes $(\frac{X}{H})_m = (\frac{X}{H})_\odot$ (see, however, Sofia & Meyer 2001). For galaxies with non-solar composition one should instead use the corresponding abundance pattern. The depletion D_x does not scale linearly with the quantity

of dust or with its chemical composition. In order to derive a scaling law we define instead the *fraction in dust*,

$$f_x = \frac{N_{x,d}}{N_{x,m}}, \quad (2)$$

where $N_{x,d}$ is the column density of atoms X in the dust and $N_{x,m}$ the column density in the medium (gas plus dust).¹ The fraction in dust is simply related to the measured depletion:

$$f_x = 1 - 10^{D_x}. \quad (3)$$

The fraction f_x must scale linearly with the amount of dust and with the abundance of X in dust. To derive this relation we express all abundances by number and relative to the abundance of an arbitrary element Y (e.g. iron). We therefore define the *abundance of X in the medium*

$$a_x = \frac{N_{x,m}}{N_{y,m}}, \quad (4)$$

and the *abundance of X in the dust*

$$p_x = \frac{N_{x,d}}{N_{y,d}}. \quad (5)$$

We also use the element Y as a reference for estimating the dust content of the system. For a given chemical composition of the dust (of the medium) the total number of atoms of metals in the dust (in the medium) will be proportional to $N_{y,d}$ (to $N_{y,m}$). Therefore we define the *dust-to-metals ratio* as

$$r = \frac{N_{y,d}}{N_{y,m}}. \quad (6)$$

This definition is free from any assumption on the extinction properties of the dust. With the above definitions the fraction in dust becomes

$$f_x = r a_x^{-1} p_x. \quad (7)$$

In previous work f_x was assumed to scale linearly with r . This is correct only if the p_x parameters are constant, i.e. if the dust composition does not

¹We consider quantities integrated along the line of sight, such as the column density, for consistency with the empirical definition (1). An identical treatment could be done using local quantities instead, such as volume densities.

vary when r varies. Here the more general situation is considered in which the abundances in the dust may depend on r and also on a_x , i.e.

$$p_x = p_x(r, a_x) \quad . \quad (8)$$

Studies of the Galactic ISM indicate that the dust-to-metals ratio is linked to the physical state of the medium. In fact clouds with similar physical properties have similar levels of depletion and depletions appear to be lower when the physical conditions become harsher (e.g. higher temperature or kinetic energy) (SS96). It is reasonable to expect that once the physical conditions of the medium are specified, also r and the dust composition characteristic of those particular physical conditions are determined. If we consider r as an indirect indicator of the physical state, then relation (8) is equivalent to assuming that *the dust composition is determined by the physical state and by the chemical composition of the medium*. This assumption is much more realistic than assuming that the dust composition is constant.

Therefore, we consider r and a_x as independent variables of our problem. By logarithmic differentiating Eq. (7) taking into account the functional dependence (8), we derive

$$\frac{df_x}{f_x} = (1 + \eta_x) \frac{dr}{r} + (\varepsilon_x - 1) \frac{da_x}{a_x} \quad , \quad (9)$$

where

$$\eta_x \equiv \frac{r}{p_x} \frac{\partial p_x}{\partial r} \quad (10)$$

and

$$\varepsilon_x \equiv \frac{a_x}{p_x} \frac{\partial p_x}{\partial a_x} \quad . \quad (11)$$

We now consider an interstellar medium i (with $r = r_i$ and $a_x = a_{x,i}$) that undergoes small variations δr and δa_x and is transformed, as a result, into a medium j (with $r = r_j$ and $a_x = a_{x,j}$). If η_x and ε_x can be considered constant during such transformation we can integrate Eq. (9) and obtain the scaling law

$$\frac{f_{x,j}}{f_{x,i}} = \left(\frac{r_j}{r_i} \right)^{(1+\eta_x)} \left(\frac{a_{x,j}}{a_{x,i}} \right)^{(\varepsilon_x-1)} \quad . \quad (12)$$

The scaling law (12), together with Eq. (1), relates variations of depletion patterns to variations

of dust-to-metals ratios and of elemental abundances. This relation has been derived mathematically, having made no assumption as to the mechanisms of dust formation, accretion and destruction. The relation holds always true for infinitesimal changes δr and δa_x . It can be applied to transformations involving discrete changes Δr and Δa_x as long as η_x and ε_x are constant during the integration of Eq. (9). Thanks to the fact that abundances in the dust p_x do not appear explicitly in the scaling law, it is not necessary to make *ad hoc* assumptions on the dust chemical composition. Instead, we must determine the parameters η_x and ε_x . In the following sections we discuss the physical meaning of such parameters and show how they can be empirically determined.

2.1. Physical meaning of the parameters η_x and ε_x

The physical meaning of η_x and ε_x can be understood by writing the definitions (10) and (11) in the following form

$$\frac{\delta p_x}{p_x} \simeq \eta_x \frac{\delta r}{r} \quad , \quad (13)$$

and

$$\frac{\delta p_x}{p_x} \simeq \varepsilon_x \frac{\delta a_x}{a_x} \quad . \quad (14)$$

Both parameters describe how sensitive the dust relative abundances p_x are to changes in the conditions of the medium. The parameter η_x indicates what percent variation of the relative abundance in the dust occurs in correspondence to a percent variation of the dust-to-metals ratio. Since r is related to the physical conditions of the medium, in practice η_x indicates how efficiently the abundance in the dust is affected by changes of the physical conditions. If $\eta_x = 0$, the relative abundance in the dust of the element X is not affected by variations of r .

The parameter ε_x indicates the percent variation of the relative abundance in the dust that occurs in correspondence to a percent variation of the relative abundance in the medium. In practice, the parameters ε_x indicate the efficiency of the mechanisms that convert a change in the composition of the medium into a change in the composition of the dust. If $\varepsilon_x = 0$, the relative abundance of X in the dust is not affected by changes in the relative abundance in the medium.

The parameters η and ε have special values, or do not need to be determined, for the reference element Y. In fact, it is easy to see from (12) that $\eta_Y = 0$ since, by definition, $f_{Y,j}/f_{Y,i} = r_j/r_i$. On the other hand, because $a_{Y,j} = a_{Y,i} = 1$, ε_Y does not need to be determined to use relation (12). In the next two sections we show how it is possible to empirically determine the parameters η_X and ε_X for the generic element X.

3. Estimate of the η_X parameters from Galactic studies

We assume that Galactic interstellar abundances are constant, at least in the solar vicinity. This implies that $a_{X,j} = a_{X,i}$ and, as a consequence, the scaling law (12) becomes

$$f_{X,j} = \left(\frac{r_j}{r_i}\right)^{(1+\eta_X)} f_{X,i} . \quad (15)$$

Given the simplified form of the scaling relation, the Galactic ISM is the ideal place to determine the parameters η_X and to probe whether they are constant or not in different environments. The fractions in dust f_X and $r = f_Y$ can be determined from the measured depletions by using Eqs.(3) and (1). By comparing the fractions in dust in two different types of clouds i and j , each type characterized by a specific depletion pattern, it is possible to derive $\eta_{X,ij} = \log(f_{X,j}/f_{X,i})/\log(r_j/r_i) - 1$. If the parameter η_X is constant for any variation of the dust-to-metals ratio, then a single value of η_X should be obtained from any pair (ij) of depletion patterns considered.

Here we consider the four types of depletion patterns discussed in SS96² (see Fig. 1). In order of decreasing depletion, these patterns are representative of (1) cool clouds in the Galactic disk, (2) warm clouds in the disk, (3) disk plus halo clouds, and (4) warm halo clouds. The lines of sight considered by SS96 also cover a significant range of extinction properties, with strength of the 217.5 nm emission bump as high as $E(\text{bump})=0.89$ in HD 24912 and as low as $E(\text{bump})=0.00$ and 0.36 in HD 38666 and HD 116852, respectively (Savage

et al. 1985). We compared pairs of the 4 SS96 depletion patterns to estimate $\eta_{X,ij}$. The results are shown in Table 1, where the quoted errors have been estimated propagating the uncertainties of the fractions in dust. For some elements the η_X values obtained from different pairs of patterns show a different behavior depending on whether the warm halo is considered or not. The η_X values obtained from cool disk, warm disk and warm disk-plus-halo patterns are in agreement for all elements considered. When we compare the warm halo with the cool and warm disk, the derived parameters for Ni, Cr and Mg are still approximately constant³. However, Mn and Si show different values, suggesting that for these elements the rate of incorporation into dust, or detachment from dust, is different when we consider the transition to halo gas.

The approximately constant values of the η_X parameters obtained for most elements over a wide range of interstellar conditions encourages us to use relation (15) for modeling all the Galactic depletion patterns. In Fig. 1 we show the results obtained using the warm disk as the i -th reference pattern. One can see that all the Galactic patterns can be matched using the set of values $\eta_{X,21}$ listed in Table 1. In spite of the lack of constancy of η_{Si} and η_{Mn} when the warm halo pattern is considered, the model is capable of fitting also the Si and Mn depletions in the warm halo within the observational errors. Therefore, relation (15) provides an empirical way to express *all* the different types of depletion patterns by varying only one parameter, r_j/r_i . This is a significant improvement with respect to previous work, in which the fractions in dust were assumed to scale linearly with r_j/r_i (i.e. $\eta_X = 0$ for all elements) and in which by no means was it possible to model at the same type different depletion patterns.

The fact that all types of Galactic depletions can be modeled with a single analytical expression suggests a continuity of the dust properties in different types of interstellar clouds, consistent with results of previous work (Joseph et al. 1986; Joseph 1988; Sofia, Cardelli & Savage 1994). The existence of specific patterns of depletions probably reflects the existence of well defined phases

²The Mg and Ni column densities and depletions considered by SS96 have been updated using revised values of the Mg II (Welty et al. 1999 and refs. therein) and Ni II (Fedchak & Lawler 1999; Howk, Savage & Fabian 1999) oscillator strengths.

³Iron is not considered since $\eta_{\text{Fe}} = 0$ in all cases by definition.

of the ISM, each one with characteristic physical parameters which determine the properties of the dust, as proposed by Spitzer (1985). However, in the transition from disk to halo gas important changes in the dust properties must occur to explain the sudden changes of η_x values. These changes are quite significant for Si, suggesting a different behavior of this element as far as its ability to be incorporated in (or detached from) dust grains in different types of interstellar environments.

4. Estimate of the ε_x parameters from extragalactic studies

If the chemical composition of the medium is not constant, it is necessary to know the ε_x parameters to apply the scaling law (12). Among the possible choices of ε_x , two values have a special meaning: $\varepsilon_x = 0$ implies that the dust composition is insensitive to variations of the overall composition; $\varepsilon_x = 1$ implies that dust composition scales in proportion to the composition of the medium, a possibility which seems logical a priori. In addition, the possibility that $\varepsilon_x = 1$ is attractive as this would imply that Galactic-type depletion patterns can be applied to studies of galaxies with different chemical compositions. In fact, when $\varepsilon_x = 1$, Eq. (12) becomes equal to Eq. (15), i.e. the depletion patterns are of Galactic type independent of any change of the chemical composition of the medium.

As in this study we are not treating the complex mechanisms of dust formation and destruction, we leave the possibility open that ε_x may take different values. We do not consider, however, values $\varepsilon_x < 0$. In fact, negative values would imply that an increase of the abundance of the element X in the medium would lead to a decrease of its abundance in the dust.

In order to constrain the parameters ε_x we must study interstellar depletions in environments with non-solar abundances. These can be found, for instance, in the ISM of external galaxies. To apply the scaling law to external galaxies we assume that any medium i with specified $r = r_i$ and $a_x = a_{x,i}$, even if located in two arbitrary galaxies A and B , is characterized by a unique dust composition, i.e. $p_x(r_i, a_{x,i})_A = p_x(r_i, a_{x,i})_B$. From this assumption, from (7) and from (12) we derive an

expression which relates the depletions of the j -th interstellar medium in the external galaxy E to the depletions of the i -th medium in our Galaxy:

$$f_{x,j} = \left(\frac{r_j}{r_i}\right)^{(1+\eta_x)} \cdot 10^{(\varepsilon_x-1)[\frac{X}{Y}]_{m,E}} \cdot f_{x,i} \quad , \quad (16)$$

where

$$\left[\frac{X}{Y}\right]_{m,E} \equiv \log\left(\frac{X}{Y}\right)_{m,E} - \log\left(\frac{X}{Y}\right)_{\odot} \quad , \quad (17)$$

$(\frac{X}{Y})_{m,E}$ is the abundance in the medium of the external galaxy, and $(\frac{X}{Y})_{\odot}$ is the abundance in the medium of our Galaxy, taken to be solar. Eq. (16) is a generalization of Eq. (11) in Vladilo (1998), which can be derived from (16) for $\eta_x = 0$ and $\varepsilon_x = 0$.

The scaling law (16) can be used to estimate the depletions in galaxies with non-solar abundances using a well-known Galactic depletion pattern as the reference pattern i . As discussed in the previous section, Galactic studies indicate that the η_x parameters can be considered approximately constant under different types of interstellar conditions, including variations of the physical state and of the strength of the 217.5 nm emission bump. This gives us confidence to use the values derived in our Galaxy for other galaxies as well, even though, in principle, the adoption of Galactic η_x values should be considered as an a priori assumption. As far as the ε_x parameters are concerned, we can probe their behavior from the study of nearby galaxies with non-solar abundances. For an external galaxy E , sufficiently close to measure the gas-phase abundances, $(\frac{X}{H})_{g,E}$, and to derive a set of reference abundances from stellar studies, $(\frac{X}{H})_{m,E}$, the depletions can be estimated from the expression

$$D_{x,E} = \left[\frac{X}{H}\right]_{g,E} - \left[\frac{X}{H}\right]_{m,E} = \left[\frac{X}{H}\right]_{g,E} - \left[\frac{Y}{H}\right]_{m,E} - \left[\frac{X}{Y}\right]_{m,E} \quad , \quad (18)$$

where the terms in square brackets are defined as in Eq. (17). It should be noted that not only the model depletions (16), but also the measured depletions (18) change according to the abundance ratios $[\frac{X}{Y}]_{m,E}$. If we know these ratios from stellar studies we can compare the observed and predicted depletions and so constrain the parameters ε_x , since we adopt η_x from Galactic studies. The

Magellanic Clouds (MCs) are ideal targets for applying this technique. A first application is presented in the next Section 4.1.

4.1. Constraints from SMC interstellar studies

Only a few lines of sight have been observed at high spectral resolution in the UV to study interstellar depletions in the MCs. We consider in this study the lines of sight to the SMC stars Sk 78, Sk 108, and Sk 155, for which interstellar column densities of several metals have been obtained from *HST* observations (Welty et al. 1997, 2001; Koenigsberger et al. 2001) and H I column densities from *IUE* observations (Fitzpatrick 1985).

To derive the observed depletions (18) we used the gas phase abundances $[X/H]_{g,SMC}$ obtained from the total SMC interstellar column densities (Table 1 in Welty et al. 2001). For the intrinsic SMC metallicity we adopted $[Fe/H]_{m,SMC} = -0.6 \pm 0.2$ dex from the typical values of SMC stellar abundances (Russell & Dopita 1992; Welty et al. 1997). This range of metallicity is in agreement with the SMC interstellar $[Zn/H]$ measurements in the same lines of sight, taking into account that Zn is modestly depleted in the Galactic ISM (Roth & Blades 1995).⁴ To derive the model depletions (16), we used the fractions in dust $f_{x,i}$ of the Galactic *warm disk* and the exponents $\eta_{x,21}$ that simultaneously fit all the Galactic ISM patterns (Fig. 1 and Table 1). All the model predictions are normalized to match the SMC iron depletions by varying the parameter r_j/r_i .

As far as the intrinsic SMC abundances $[X/Fe]_{m,SMC}$ are concerned, we first considered the case of solar ratios and then a few non-solar abundance patterns discussed below. In all cases we obtain $r_j/r_i = 0.930, 0.802$, and 1.020 for the sight lines to Sk 78, Sk 108, and Sk 155, respectively. These values of r_j/r_i are in the range typical of Galactic *warm halo*, *warm disk+halo*, and *cold disk* clouds, respectively (compare with the r_j/r_i values in the caption to Fig. 1), in agreement with the conclusions pointed out by Welty et al. (1997, 2001).⁵

For the case of solar ratios, i.e. $[X/Fe]_{m,SMC} = 0$, the results for the sight lines to Sk 78, Sk 108, and Sk 155 are shown in Figs. 2, 3, and 4, respectively. One can see that the predicted depletions do not fit well the observed ones. In particular, the Si and Mg measurements tend to lie above the predictions while the opposite is true for Mn and Ni. These disagreements cannot be attributed to the uncertainty of the metallicity level. In fact, similar results are found adopting $[Fe/H]_{m,SMC} = -0.8$ dex, and $[Fe/H]_{m,SMC} = -0.4$ dex, the two extreme values of SMC metallicity still consistent with stellar data.

The systematic deviations between observed and predicted depletions suggest that the SMC depletion patterns are peculiar and/or that the SMC relative abundances are non solar. Welty et al. (2001) suggested that the SMC dust may be essentially free of Si and Mg, particularly in the line of sight to Sk 155 where they find exceedingly high $[Si/Zn]$ and $[Mg/Zn]$ ratios. These authors made their analysis assuming solar SMC abundance ratios. In the present work we consider, in addition, the possibility that the SMC abundances have modest deviations from solar ratios.

The SMC abundance pattern is rather uncertain. In Table 2 we list average abundance ratios derived from SMC stellar studies, taken from Russell & Dopita (1992), Hill (1997), and Venn (1999). The observational spread is high and the measurements are often consistent with solar values (Welty et al. 1997). However, tentative evidence of departures from solar ratios is present in the data. In fact, small departures are expected at the metallicity of the SMC. For instance, Milky Way stars with metallicities $[Fe/H] \simeq -0.6$ dex do show characteristic non solar ratios that we also list in Table 2 (from Ryan, Norris & Beers 1996; RNB96). An enhancement of the α/Fe ratios $[Si/Fe]$ and $[Mg/Fe]$ and an underabundance of the $[Mn/Fe]$ ratio are present in metal-poor Galactic stars. Even if the SMC has probably undergone a chemical evolution different from that of the Milky Way, we still expect to find a hint of similar deviations in the SMC abundance pattern. For instance, if the chemical evolution has proceeded with a lower rate of (or

155, while only the total SMC column densities are considered here.

⁴In the present paper we do not consider the detailed behavior of Zn depletion because this element is not included in the "standard" depletion patterns given by SS96.

⁵In addition, Welty et al. (2001) studied the multi-component structure of the SMC absorptions toward Sk

a more episodic) star formation, the deviations of the α/Fe ratios are probably less marked, but still present (Matteucci 1991).

Since modest departures from solar ratios are consistent with SMC stellar data and are expected from the comparison with Galactic stars, it is worth examining if such departures can explain the peculiarities of the SMC depletion patterns. To probe this possibility we adopted the SMC abundance pattern A in Table 2 that was chosen (1) to be consistent with the SMC stellar data and (2) to deviate from solar ratios in the same sense of metal-poor Galactic stars, but by a conservatively low amount. The results obtained adopting the abundance pattern A to represent $[\text{Fe}/\text{Y}]_{\text{m,SMC}}$ are shown in Figs. 5, 6, and 7 for the sight lines to Sk 78, Sk 108, and Sk 155, respectively. In each case, three different values of ε_x were considered, namely $\varepsilon_x = 0, 1$, and 2 . For $\varepsilon_x = 1$, the agreement between observed and predicted depletions is better than in the case of intrinsic solar ratios. For instance, the Si depletion is reproduced within the errors for Sk 78 and Sk 108. However discrepancies are still present for other elements, especially in the sight-line to Sk 155. For ε_x somewhat below unity the predictions are in agreement with the observations. In fact, all the three depletion patterns, including the peculiar one towards Sk 155, can be simultaneously fit with $0 < \varepsilon_x < 1$ for most elements considered.⁶ For $\varepsilon_x = 2$, the discrepancies are even larger than in the case of solar ratios.

The depletions predicted for $\varepsilon_x \neq 1$ tend to jump to values much lower or higher than the observed depletions. In some cases $\varepsilon_x \neq 1$ all the atoms of an element are predicted to be in dust (Figs. 5 and 7). The curves obtained for $\varepsilon_x = 1$ do not suffer from this inconvenience. In addition, the case $\varepsilon_x = 1$ is attractive for the reasons explained above (Section 4, first paragraph). We therefore searched for a set of SMC relative abundances able to reproduce the observed depletions while keeping $\varepsilon_x = 1$ fixed for all elements. By trial and error we find that the abundance pattern B in Table 2 fits all elements reasonably well. The results for the sightlines to Sk 78, Sk 108, and Sk

155 are shown in Figs. 8, 9, and 10, respectively. It is encouraging that a single set of abundances is able to simultaneously fit the depletions observed in all the three lines of sight with Galactic type depletion patterns (i.e. with $\varepsilon_x = 1$). However, at the present time, some of the ratios of the abundance pattern B seem difficult to reconcile with SMC stellar data.

In conclusion, it is not possible to model the SMC depletions if the SMC abundances are strictly solar. We have two choices in modeling the observed depletions: (1) modest departures from solar values (pattern A in Table 2) and $0 < \varepsilon_x \leq 1$; (2) "Galactic type" depletions for all elements ($\varepsilon_x = 1$), but larger departures from solar ratios (pattern B in Table 2). Values of ε_x in excess of unity give depletion patterns inconsistent with the observations.

5. Summary and conclusions

An analytical expression has been derived that allows dust depletions to be estimated in interstellar environments characterized by a wide range of chemical and physical properties. In practice, the depletions are estimated as a function of the dust-to-metals ratio, r , and of the relative abundance of the element X in the medium, a_x , by scaling a depletion pattern chosen as a reference. The scaling law, given in Eq. (12), has been derived making no assumption on the mechanisms of dust formation, accretion or destruction. No hypothesis has been made on the extinction properties of the dust. The functional form (12) is always valid for infinitesimal changes δr and δa_x . For finite changes Δr and Δa_x the expression is valid if the parameters η_x and ε_x are constant. These parameters are essentially derivatives of the relative abundance of the element X in the dust, p_x . In practice, the parameters η_x indicate how the chemical composition of the dust is affected by changes of the dust-to-metals ratio r . The parameters ε_x indicate how the composition of the dust is affected by changes in the composition of the medium.

The scaling law can be applied to interstellar clouds of our Galaxy and of external galaxies with solar or non-solar abundances — including Damped Ly α systems — once the sets of parameters η_x and ε_x are determined. The assumption required to apply the scaling law to external galax-

⁶The results for Ni depletions do not improve with respect to the case of solar ratios because in the abundance pattern A we adopt $[\text{Ni}/\text{Fe}] = 0$.

ies is that the dust chemical composition is a function of r and a_x valid in any type of interstellar medium. This assumption is much more realistic than assumptions previously adopted in studies of DLA systems, in which depletion patterns were estimated using specific types of Galactic dust.

The parameters η_x and ε_x can be determined empirically by comparing observed depletion patterns in interstellar media with different physical and chemical properties. We have used the typical Milky Way depletion patterns to estimate the parameters η_x in environments with variable r but constant (solar) abundances. The resulting values of η_x are approximately constant for most elements in a wide range of physical conditions, supporting the validity of the scaling law (12), at least as far as the dependence on r is concerned. With the derived set of η_x parameters, the scaling law is able to simultaneously fit all the typical Milky Way depletion patterns by only varying r .

The parameters ε_x can be determined empirically by studying interstellar depletions of galaxies with known abundances different from the solar ones. We have applied this technique to the SMC, for which the intrinsic abundances are constrained from stellar studies and depletion data are available for three lines of sight. The observed SMC depletions can be modeled with the scaling law if the SMC abundance ratios are slightly non solar. The required departures from solar ratios are consistent with the results of SMC stellar studies and with expectations based on Galactic stellar abundances of stars having the same metallicity of the SMC. The agreement between observed and predicted depletions is obtained at values $\varepsilon_x \simeq 1$ or somewhat below unity. With this choice of parameters the scaling law is able to simultaneously fit the three available SMC depletion patterns, including the anomalous pattern observed toward Sk 155. Values $\varepsilon_x > 1$ are excluded by the present analysis. The uncertainty of the SMC stellar abundances prevent firmer conclusions or more constrained ε_x values.

The capability of the scaling relation presented here to match Galactic and SMC depletion patterns is rather encouraging. To probe the general validity of the scaling law it is desirable to measure depletions in a larger number of extragalactic lines of sight. However, these studies will yield stringent constraints only if the intrinsic abundances of the

external galaxies, mostly based on stellar observations, will be determined with accuracy. A major step in this direction can be made in the next few years by observing a relatively large number of stars of the Magellanic Clouds at high spectral resolution. These time-consuming efforts will be rewarded by the possibility of modeling interstellar depletions and deriving dust-corrected abundances in high redshift galaxies observed as QSO absorption systems. An implementation of the scaling relation for deriving dust-corrected abundances in Damped Ly α systems will be presented in a separate paper.

I wish to thank Daniel Welty an anonymous referee for suggestions that have improved the present work.

REFERENCES

- Anders, E., & Grevesse, N. 1989, *Geochim. Cosmochim. Acta*, 53, 197
- Centuriòn, M., Bonifacio, P., Molaro, P., & Vladilo, G. 2000, *ApJ*, 536, 540
- Fedchak, J.A., & Lawler, J.E. 1999, *ApJ*, 523, 734
- Fitzpatrick, E.L. 1985, *ApJS*, 59, 77
- Hill, V. 1997, *A&A*, 324, 435
- Hou, J.L., Boissier, S., Prantzos, N. 2001, *A&A*, 370, 23
- Howk, J.C., & Savage, B.D., & Fabian, D. 1999, *ApJ*, 525, 253
- Jenkins, E.B., Savage, B.D., & Spitzer L., Jr. 1986, *ApJ*, 301, 355 (JSS86)
- Joseph, C.L., 1988, *ApJ*, 335, 157
- Joseph, C.L., Snow, T.P., Seab, C.G., & Crutcher, R.M. 1986, *ApJ*, 309, 771
- Koenigsberger, G., Georgiev, L., Peimbert, M., Walborn, N.R., Barbá, R., Niemela, V.S., Morrell, N., Tsvetanov, Z., Schulte-Ladbeck, R. 2001, *AJ*, 121, 267
- Kulkarni, V.P., Fall, S.M., & Truran, J.W. 1997, *ApJ*, 484, L7

- Lauroesch, J.T., Truran, J.W., Welty, D.E., & York, D.G. 1996, *PASP*, 108, 641
- Lu, L., Sargent, W.L.W., & Barlow, T.A. 1996, *ApJS*, 107, 475
- Matteucci, F. 1991, in *SN1987A and other Supernovae*, eds. I.J. Danziger & K.Kjar, *ESO Proc.* 37, (Garching: ESO), 703
- Molaro, P., Bonifacio, P., Centuri3n, M., D’Odorico, S., Vladilo, G., Santin, P., Di Marcantonio, P. 2000, *ApJ*, 541, 54
- Morton, D.C. 1974, *ApJ*, 193, L35
- Pettini, M., Ellison, S.L., Steidel, C.C., Shapley, A.E., & Bowen, D.V. 2000, *ApJ*, 532, 65
- Pettini, M., King, D.L., Smith, L.J., & Hunstead, R.W. 1997, *ApJ*, 478, 536
- Pettini, M., Smith, L.J., Hunstead, R.W. & King, D.L. 1994, *ApJ*, 426, 79
- Prochaska, J.X., & Wolfe, A.M. 1999, *ApJS*, 121, 369
- Prochaska, J.X., & Wolfe, A.M. 2002, *ApJ*, in press, (astro-ph/0110351)
- Roth, K.C., & Blades, C., 1995, *ApJ*, 445, L95
- Russell, S.C., & Dopita, M.A. 1992, *ApJ*, 384, 508
- Ryan, S.G., Norris, J.E., & Beers, T.C. 1996, *ApJ*, 471, 254
- Savage, B.D., Massa, D., Meade, M., Wesselius, P.R. 1985, *ApJS*, 59, 397
- Savage, B.D., & Sembach, K.R. 1996, *ARA&A*, 34, 279 (SS96)
- Savaglio, S., Panagia, N., & Stiavelli, M. 2000, *ASP Conf. Ser.* 215, 65
- Sofia, U.J., Cardelli, J.A., & Savage, B.D. 1994, *ApJ*, 430, 650
- Sofia, U.J., & Meyer, D.M. 2001, *ApJ*, 554, L221
- Spitzer, L. 1978, *Physical Processes in the Interstellar Medium*, (New York: Wiley Interscience)
- Spitzer, L. 1985, *ApJ*, 290, L21
- Tielens, A.G.G.M., Allamandola, L.J. 1987, in *Interstellar Processes*, ed. D.J. Hollenbach & H.A. Thronson, (Dordrecht: Reidel), 533
- Venn, K.A. 1999, *ApJ*, 518, 405
- Vladilo, G. 1998, *ApJ*, 493, 583
- Vladilo, G., Bonifacio, P., Centuri3n, M., & Molaro, P. 2000, *ApJ*, 543, 24
- Welty, D.E., Hobbs, L.M., Lauroesch, J.T., Morton, D.C., Spitzer, L., & York, D. 1999, *ApJS*, 124, 465
- Welty, D.E., Lauroesch, J.T., Blades J.C., Hobbs, L.M., & York, D.G. 1997, *ApJ*, 489, 672
- Welty, D.E., Lauroesch, J.T., Blades J.C., Hobbs, L.M., & York, D.G. 2001, *ApJ*, 554, L75

TABLE 1
EMPIRICAL DETERMINATION OF THE η_x PARAMETERS^a

X	$\eta_{x,21}$	$\eta_{x,31}$	$\eta_{x,32}$	$\eta_{x,42}$	$\eta_{x,41}$
Si	$+4.68 \pm 1.77^b$	$+5.27 \pm 0.60$	$+5.78 \pm 1.89^b$	$+0.87 \pm 2.53^b$	$+1.70 \pm 1.94$
Mg	$+3.60 \pm 1.50$	$+3.48 \pm 0.35$	$+3.37 \pm 1.29$	$+3.46 \pm 3.98$	$+3.49 \pm 3.10$
Mn	$+0.53 \pm 0.41$	$+0.69 \pm 0.27$	$+0.82 \pm 0.60$	-0.18 ± 0.51	-0.02 ± 0.39
Cr	$+0.37 \pm 0.20$	$+0.37 \pm 0.29$	$+0.36 \pm 0.56$	$+0.45 \pm 0.66$	$+0.43 \pm 0.52$
Fe	$+0.00 \pm 0.07$	$+0.00 \pm 0.32$	$+0.00 \pm 0.59$	$+0.00 \pm 0.19$	$+0.00 \pm 0.15$
Ni	$+0.01 \pm 0.11$	$+0.02 \pm 0.13$	$+0.03 \pm 0.26$	$+0.03 \pm 0.21$	$+0.02 \pm 0.17$

^a Each parameter η_x is derived from relation (15) by comparing the fractions in dust of the corresponding element in two different types of Galactic depletion patterns. The fraction in dust is estimated from relation (3). The two indices of each parameter indicate which pair of depletion patterns is considered. The indices correspond to: (1) cool disk, (2) warm disk, (3) warm disk+halo, (4) warm halo. The parameters are normalized in such a way that $\eta_{\text{Fe}} = 0$ for any pair of depletion patterns considered. The parameters $\eta_{x,34}$ are not estimated because the depletion patterns (3) and (4) are almost overlapping within the errors.

^b $D_{\text{Si}} = -0.51$ dex adopted for the warm disk depletion of Si. This choice of D_{Si} , which lies in the range given by SS96, gives a better simultaneous fit of all the depletion patterns.

TABLE 2
ABUNDANCE RATIOS IN METAL-POOR GALACTIC STARS AND IN THE SMC

	RNB96 ^a	RD92 ^b	H97 ^c	V99 ^d	A	B
[Si/Fe]	+0.19	+0.15 ± 0.22	−0.14 ± 0.19	+0.26 ± 0.19	+0.10	+0.15
[Mg/Fe]	+0.12	+0.07 ± 0.18	+0.16 ± 0.22	−0.01 ± 0.12	+0.10	+0.10
[Mn/Fe]	−0.30	+0.17 ± 0.34	−0.10	−0.25
[Cr/Fe]	−0.02	+0.09 ± 0.24	−0.31 ± 0.18	−0.02 ± 0.13	+0.00	+0.00
[Ni/Fe]	+0.00	+0.27 ± 0.24	−0.38 ± 0.14	...	+0.00	−0.10

^a Abundances of metal-poor Milky Way stars at metallicity $[\text{Fe}/\text{H}] \simeq -0.6$ dex. Values taken in correspondence of the "midmean vector" defined by Ryan et al. (1996).

^b From Table 1 by Russell & Dopita (1992), corrected when necessary for the meteoritic solar abundances by Anders & Grevesse (1989). The abundances are relative to Galactic stars of same spectral type.

^c Average values of 6 K-type supergiants in the SMC (Hill 1997; Table 3). Mg measured only in 3 stars.

^d Average values of 10 A-type supergiants in the SMC (Venn 1999; Table 6). Only measurements of singly ionized species have been considered. The abundances are relative to Galactic A-type supergiants.

NOTE.— Solar ratios taken from the meteoritic values by Anders & Grevesse (1989). The errors have been computed propagating the errors of each of the two elements considered in the ratio.

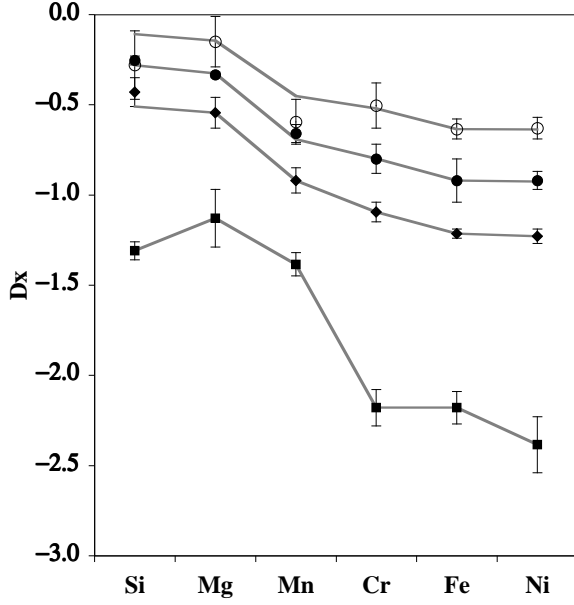


Fig. 1.— Comparison of observed and predicted interstellar depletion patterns in the Galaxy. Symbols: Galactic patterns observed in the *cool disk* (squares), the *warm disk* (diamonds), the *warm disk plus halo* (filled circles), and the *warm halo* (empty circles), from Table 6 in SS96. Lines: model predictions obtained from the scaling law (15), derived using the *warm disk* as the reference depletion pattern and normalized to fit the observed Fe depletions using the values $r_1/r_2 = 1.058$, $r_3/r_2 = 0.935$, and $r_4/r_2 = 0.840$; the parameters η_x are taken from Table 1 ($\eta_{x,21}$).

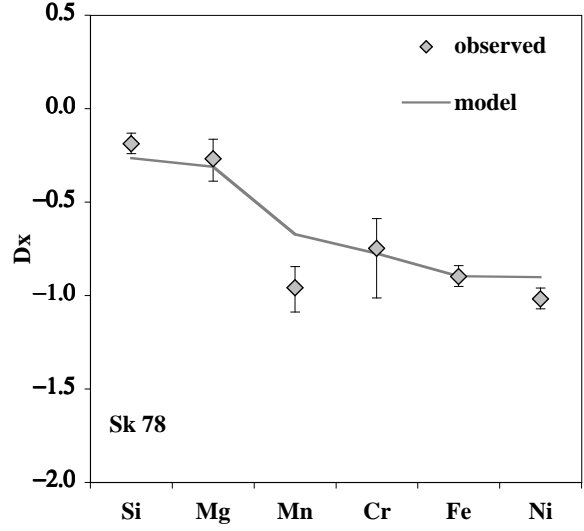


Fig. 2.— Observed and predicted SMC depletion patterns in the line of sight to Sk 78 derived from Eqs. (18) and (16), respectively, for the case of solar $[X/Fe]_{\text{ref,SMC}}$ ratios. Symbols: observed depletions obtained using the SMC column densities by Welty et al. (2001), $\log N(\text{H I})_{\text{SMC}} = 20.93 \pm 0.05$ (Fitzpatrick 1985), and $[Y/H]_{\text{ref,SMC}} = -0.6$ dex. Line: predicted depletions obtained using the Galactic *warm disk* as the reference pattern, $r_j/r_i = 0.930$, and the parameters $\eta_{x,21}$ (see Table 1 and Fig. 1).

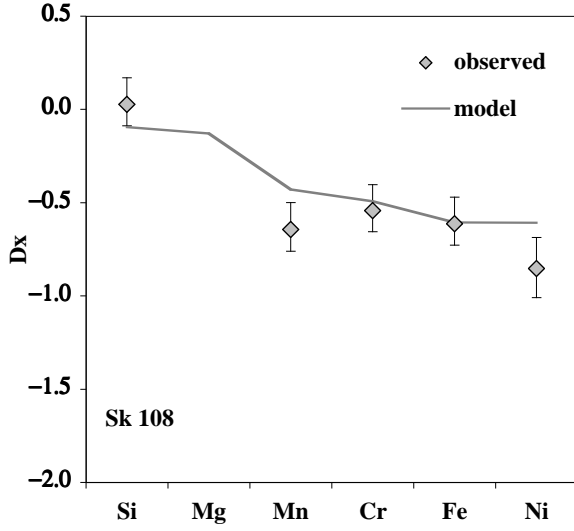


Fig. 3.— Observed and predicted SMC depletion patterns in the line of sight to Sk 108 derived from Eqs. (18) and (16), respectively, for the case of solar $[X/Fe]_{\text{ref,SMC}}$ ratios. Symbols: observed depletions obtained using the SMC column densities by Welty et al. (2001), $\log N(\text{H I})_{\text{SMC}} = 20.54^{+0.11}_{-0.14}$ (Fitzpatrick 1985), and $[Y/H]_{\text{ref,SMC}} = -0.6$ dex. Line: predicted depletions obtained using the Galactic *warm disk* as the reference pattern, $r_j/r_i = 0.802$, and the parameters $\eta_{x,21}$ (see Table 1 and Fig. 1).

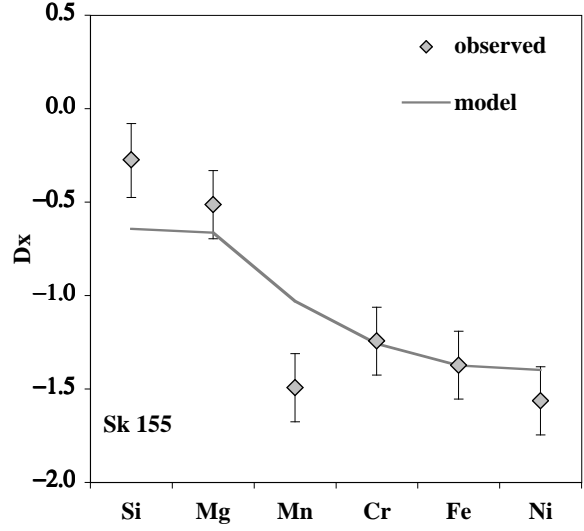


Fig. 4.— Observed and predicted SMC depletion patterns in the line of sight to Sk 155 derived from Eqs. (18) and (16), respectively, for the case of solar $[X/Fe]_{\text{ref,SMC}}$ ratios. Symbols: observed depletions obtained using the SMC column densities by Welty et al. (2001), $\log N(\text{H I})_{\text{SMC}} = 21.54 \pm 0.18$ (Fitzpatrick 1985), and $[Y/H]_{\text{ref,SMC}} = -0.6$ dex. Line: predicted depletions obtained using the Galactic *warm disk* as the reference pattern, $r_j/r_i = 1.020$, and the parameters $\eta_{x,21}$ (see Table 1 and Fig. 1).

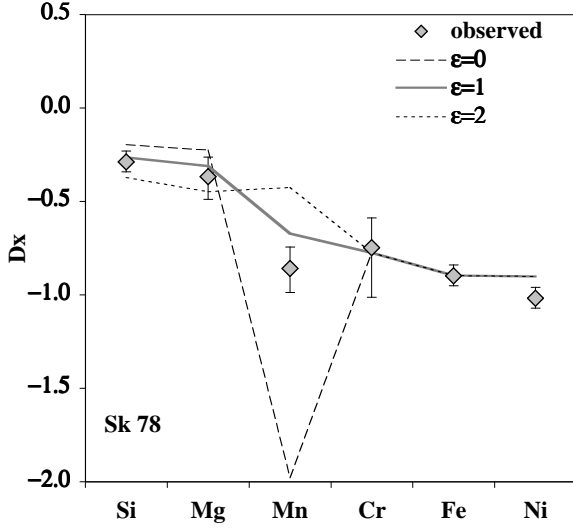


Fig. 5.— Observed and predicted SMC depletions toward Sk 78. Same as in Fig. 2, but with non solar $[X/Fe]_{\text{ref,SMC}}$ ratios (abundance pattern "A" in Table 2). Lines: depletions predicted for different values of ε_x . Dashed line: $\varepsilon_x = 0$. Thick line: $\varepsilon_x = 1$. Dotted line: $\varepsilon_x = 2$. For $\varepsilon_{\text{Mn}} = 0$ all the atoms of Mn are predicted to be in dust; a conventional value $D_{\text{Mn,SMC}} = -2$ dex is plotted in the figure.

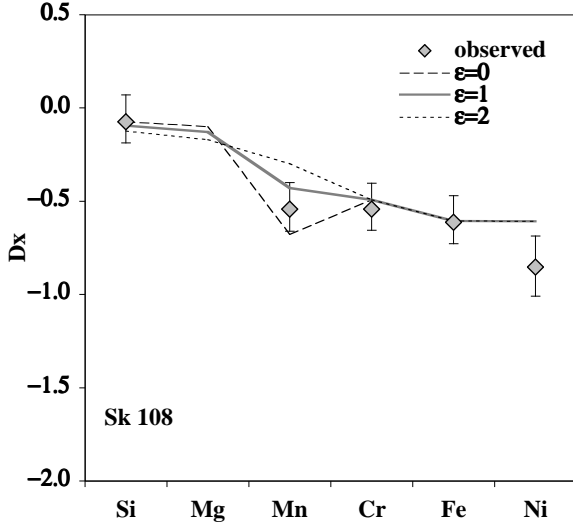


Fig. 6.— Observed and predicted SMC depletions toward Sk 108. Same as in Fig. 3, but with non solar $[X/Fe]_{\text{ref,SMC}}$ ratios (abundance pattern "A" in Table 2). Lines: depletions predicted for different values of ε_x . Dashed line: $\varepsilon_x = 0$. Thick line: $\varepsilon_x = 1$. Dotted line: $\varepsilon_x = 2$.

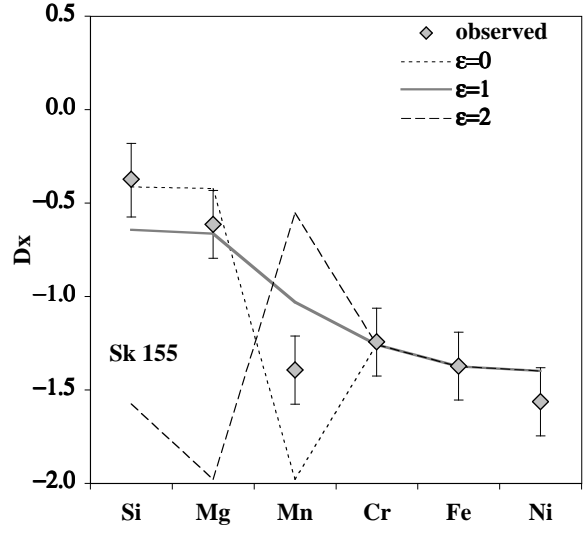


Fig. 7.— Observed and predicted SMC depletions toward Sk 155. Same as in Fig. 4, but with non solar $[X/Fe]_{\text{ref,SMC}}$ ratios (abundance pattern "A" in Table 2). Lines: depletions predicted for different values of ε_x . Dashed line: $\varepsilon_x = 0$. Thick line: $\varepsilon_x = 1$. Dotted line: $\varepsilon_x = 2$. For $\varepsilon_{\text{Mn}} = 0$ and $\varepsilon_{\text{Mg}} = 2$ all the atoms of Mn and Mg are predicted to be in dust; conventional values $D_{\text{Mn,SMC}} = D_{\text{Mg,SMC}} = -2$ dex are plotted in the figure.

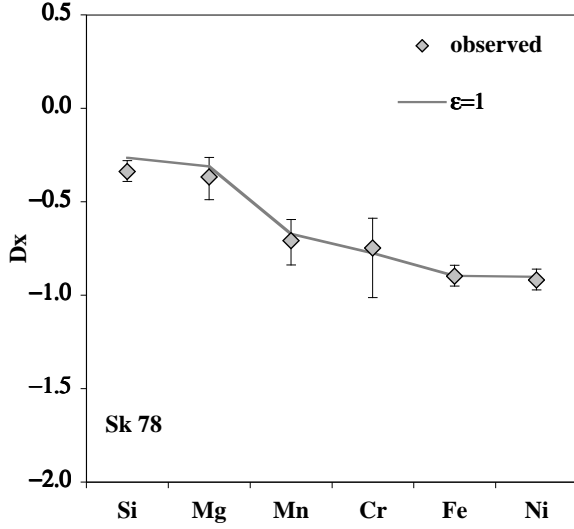


Fig. 8.— Observed and predicted SMC depletions toward Sk 78. Same as in Fig. 2, but with non solar $[X/Fe]_{\text{ref,SMC}}$ ratios (abundance pattern "B" in Table 2). Thick line: depletions predicted for $\epsilon_x = 1$.

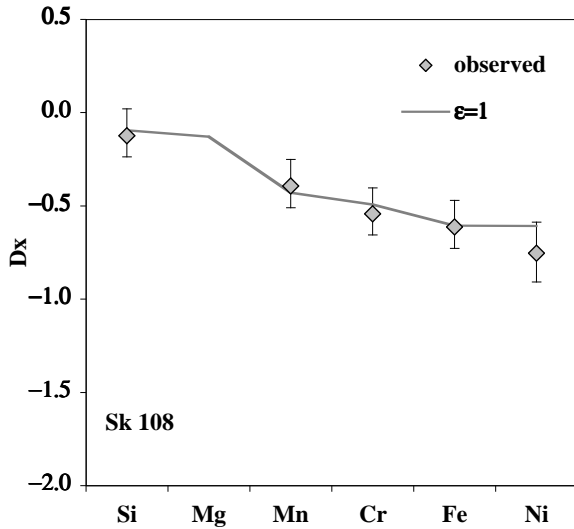


Fig. 9.— Observed and predicted SMC depletions toward Sk 108. Same as in Fig. 3, but with non solar $[X/Fe]_{\text{ref,SMC}}$ ratios (abundance pattern "B" in Table 2). Thick line: depletions predicted for $\epsilon_x = 1$.

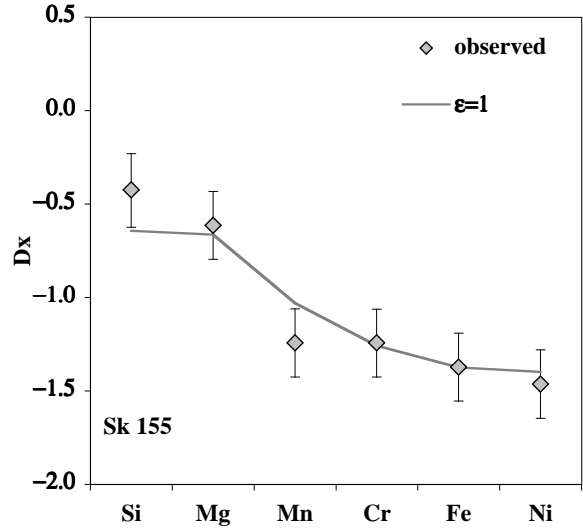


Fig. 10.— Observed and predicted SMC depletions toward Sk 155. Same as in Fig. 4, but with non solar $[X/Fe]_{\text{ref,SMC}}$ ratios (abundance pattern "B" in Table 2). Thick line: depletions predicted for $\epsilon_x = 1$.